Contribution from the Departments of Chemistry, University of Sassari, Sassari, Italy, and Northwestern University, Evanston, Illinois 60208

Vibrational Frequencies Associated with the Carbide Ligand in Iron Butterfly Clusters

P. L. Stanghellini,*[1a] M. J. Sailor,[1b] P. Kuznesof,[1b] K. H. Whitmire,[1b] J. A. Hriljac,[1b] J. W. Kolis,[1b] Y. Zheng,[1b] and D. F. Shriver*[1b]

Received February 18, 1987

The vibrational frequencies associated with the exposed carbon atom in several tetranuclear iron carbide clusters with a butterfly arrangement of atoms were investigated by infrared and Raman spectroscopy. Vibrational assignments were confirmed in most cases by ^{13}C labeling of the carbide carbon atom. The characteristic feature of the iron butterfly carbides is a readily observed band in the infrared spectrum around 900 cm^{-1}. An approximate normal-coordinate analysis on these molecules yields values of the metal–carbon force constant of about 250 N m^{-1}.

Introduction

The chemistry of organometallic carbide clusters took a new direction with the discovery of butterfly clusters containing an exposed carbide ligand.[2] Unlike the previous cluster carbides, the new clusters possess reactivity at the carbon atom.[3-5] Low-coordinate carbides are often proposed as reactive intermediates in surface chemistry,[6] and molecular clusters with exposed carbides provide models for the carbon atom in a low-coordinate metal environment on metal surfaces.[7]

Previous vibrational spectroscopic characterization of metal cluster carbides has been confined to species lacking reactivity at the carbide ligand.[8-17] These are generally high-nuclearity clusters in which the carbide ligand occupies an interstitial site; therefore, the lack of observed reactivity of such an enclosed carbon atom is not surprising. In contrast, the tetranuclear carbide cluster $[Fe_4C(CO)_{12}]^{2-}$ displays reactivity with alkylating agents or proton sources at the carbon atom,[4] consistent with the idea that lowering the steric constraints about the carbon atom enhances its reactivity.[18] In the present research, we have investigated the vibrational spectroscopy of several tetranuclear metal carbide clusters. The frequencies and assignments should prove useful for the characterization of molecular metal cluster carbides and reactive surface carbides. Force constants derived from these data are useful in the calculation of steric interactions in butterfly carbides by molecular mechanics methods.[18]

Experimental Section

Samples of $[Fe_4C(CO)_{12}]^{2-}$,[19] $[HFe_4C(CO)_{12}]^-$,[20] $Fe_4C(CO)_{13}$,[21] $HFe_4(CH)(CO)_{12}$,[20] $[Fe_3RhC(CO)_{12}]^-$,[22] and $[Fe_3WC(CO)_{13}]^{2-}$[27] were prepared according to published procedures. Selective ^{13}C enrichment at the carbide carbon of the tetrairon clusters was accomplished by enriching the carbonyls in the starting material $[Fe_4(CO)_{13}]^{2-}$ to ca. 60% in ^{13}CO.[23] Since the carbide atom is derived from a carbonyl ligand on the starting material,[19] this leads to a product that is ^{13}C enriched at all carbon atoms in the cluster. One of the ^{13}CO ligands was cleaved to produce a ^{13}C carbide ligand, and then the carbonyl ligands were exchanged by stirring a CH_2Cl_2 solution of the compound under an atmosphere of ^{12}CO for 8 days, intermittently replacing the atmosphere over the solution with fresh ^{12}CO. This final material was ^{13}C-enriched exclusively at the carbide ligand, thus simplifying the assignment of modes associated with the C ligand.

Infrared spectra were obtained on a Perkin-Elmer 580 infrared spectrometer or a Nicolet 7199 FT-IR spectrometer on Nujol mulls or CsI pellets of the samples. Low-temperature spectra were obtained on samples in a standard optical cryostat. Raman data were determined with a Spex 1401 double monochromator using 676- or 647-nm Kr ion laser excitation. A 180° backscattering technique was employed on spinning samples.[24] Laser power measured at the sample was typically 30 mW, and the band-pass of the spectrometer was approximately 5 cm^{-1}. Semiquantitative depolarization ratios were measured as described elsewhere.[25]

Results and Discussion

Vibrational Assignments for Clusters with C_{2v} Symmetry. For the idealized C_{2v} symmetry of the butterfly carbides there are four modes associated with vibrations of the carbon atom, shown schematically in Figure 1. All of these vibrations are both Raman- and IR-active. The $A_1(1)$ symmetry coordinate involves motion of the heavy atoms, and the frequency of the associated normal mode is expected to be low. The most intense band in the Raman spectrum of $[Fe_4C(CO)_{12}]^{2-}$ is at 272 cm^{-1} (Figure 2) and is assigned to this totally symmetric Fe–C–Fe stretch, which involves very little C motion because the Fe–C–Fe array is nearly linear (176°). The assignment of this band to an A_1 mode is firmly established by the observation that it is polarized in the solution Raman spectrum of $[PPN]_2[Fe_4C(CO)_{12}]$. The M–M stretching frequencies are observed in the Raman spectrum below 220 cm^{-1}.

The remaining three modes, which primarily involve motion of the carbon atom, are expected to have IR and Raman transitions between 950 and 550 cm^{-1}. In most cases these are readily observed in the infrared spectrum. As shown in Figure 3, there

(1) (a) University of Sassari. (b) Northwestern University.
(2) Bradley, J. S. *Adv. Organomet. Chem.* **1983**, *22*, 1.
(3) Bradley, J. S.; Ansell, G. B.; Hill, E. W. *J. Am. Chem. Soc.* **1979**, *101*, 7417.
(4) Holt, E. M.; Whitmire, K. H.; Shriver, D. F. *J. Am. Chem. Soc.* **1982**, *104*, 5621.
(5) Tachikawa, M.; Muetterties, E. L. *J. Am. Chem. Soc.* **1980**, *102*, 4541.
(6) Biloen, P.; Helle, J. N.; Sachtler, W. M. H. *J. Catal.* **1979**, *58*, 95.
(7) Tachikawa, M.; Muetterties, E. L. *Prog. Inorg. Chem.* **1981**, *28*, 301.
(8) Braye, E. H.; Dahl, L. F.; Hübel, W.; Wampler, D. L. *J. Am. Chem. Soc.* **1962**, *84*, 4633.
(9) Bor, G.; Stanghellini, P. L. *J. Chem. Soc., Chem. Commun.* **1979**, 886.
(10) Bor, G.; Dietler, U. K.; Stanghellini, P. L.; Gervasio, G.; Rossetti, R.; Sbrignadello, G.; Battiston, G. A. *J. Organomet. Chem.* **1981**, *213*, 277.
(11) Stanghellini, P. L.; Rossetti, R.; D'Alfonso, G.; Longoni, G., private communication.
(12) Oxton, I. A.; Kettle, S. F. A.; Jackson, P. F.; Johnson, B. F. G.; Lewis, J. *J. Mol. Struct.* **1981**, *71*, 117.
(13) Oxton, I. A.; Powell, D. B.; Goudsmit, R. J.; Johnson, B. F. G.; Lewis, J.; Nelson, W. J. H.; Nicholls, J. N.; Rosales, M. J.; Vargas, M. D.; Whitmire, K. H. *Inorg. Chim. Acta* **1982**, *64*, L259.
(14) Johnson, B. F. G.; Lewis, J.; Nicholls, J. N.; Oxton, I. A.; Raithby, P. R.; Rosales, M. J. *J. Chem. Soc., Chem. Commun.* **1982**, 289.
(15) Creighton, J. A.; Della Pergola, R.; Heaton, B. T.; Martinengo, S.; Strona, L.; Willis, D. A. *J. Chem. Soc., Chem. Commun.* **1982**, 864.
(16) Kolis, J. W.; Basolo, F.; Shriver, D. F. *J. Am. Chem. Soc.* **1982**, *104*, 5626.
(17) Stanghellini, P. L.; Cognolato, L.; Bor, G.; Kettle, S. F. A. *J. Crystallogr. Spectrosc. Res.* **1983**, *13*, 127.
(18) Bogdan, P. L.; Horwitz, C. P.; Shriver, D. F. *J. Chem. Soc., Chem. Commun.* **1986**, 553.
(19) Ceriotti, A.; Chini, P.; Longoni, G.; Piro, G. *Gazz. Chim. Ital.* **1982**, *112*, 353.
(20) Holt, E. M.; Whitmire, K. H.; Shriver, D. F. *J. Organomet. Chem.* **1981**, *213*, 125.
(21) Bradley, J. S.; Ansell, G. B.; Leonowicz, M. E.; Hill, E. W. *J. Am. Chem. Soc.* **1981**, *103*, 4968.
(22) Hriljac, J. A.; Swepston, P. N.; Shriver, D. F. *Organometallics* **1985**, *4*, 158.
(23) Drezdzon, M. A.; Shriver, D. F. *J. Mol. Catal.* **1983**, *21*, 81.
(24) Strommen, D. P.; Nakamoto, K. *Laboratory Raman Spectroscopy*; Wiley: New York, 1984; p 57.
(25) Reference 24, pp 88–89.
(26) Wilson, E. B.; Decius, J. C.; Cross, P. C. *Molecular Vibrations*; McGraw-Hill: New York, 1955.

0020-1669/87/1326-2950$01.50/0

Table I. Carbide Vibrational Data for Molecules of C_{2v} Symmetry (cm^{-1})[a]

compd	temp, K		B_2		$A_1(2)$		B_1[b]		$A_1(1)$[c]
			^{12}C	^{13}C	^{12}C	^{13}C	^{12}C	^{13}C	^{12}C
$[PPN]_2[Fe_4C(CO)_{12}]$	300	obsd	929	896	666	652	608	601	272
		calcd	931	898	673	650	590	572	290
	100	obsd	934	901	670	[660, 655]	611	606	
		calcd	935	902	673	651	591	573	291
$[PPN][HFe_4C(CO)_{12}]$	300	obsd	922	889	661	648		600	269
		calcd	923	891	665	643	592	573	287
	100	obsd	[928, 922]	893	[664, 658]	649	~609	602	
		calcd	926	893	667	645	593	574	288
$Fe_4C(CO)_{13}$	300	obsd	928	895	658	645			252
		calcd	930	897	667	645	568	550	290
	100	obsd	936	904	663	650	601	586	
		calcd	937	904	666	644	587	550	292

[a] Vaseline mulls. Those bands observed to split at low temperature are enclosed in brackets. Calculated values were obtained by a least-squares fit of the B_2 and $A_1(2)$ symmetry modes as described in the text. Both ^{12}C and ^{13}C data were used in the fit. [b] Measured by difference spectrum. [c] Obtained from the Raman spectrum as polycrystalline samples. All other data are from infrared measurements.

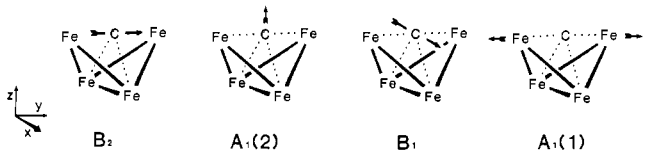

Figure 1. Schematic representation in approximate symmetry coordinates of the vibrational modes of the carbide atom in a butterfly cluster. The idealized symmetry is C_{2v}.

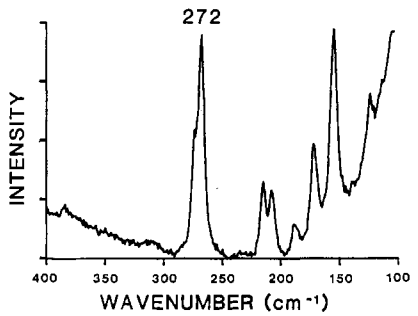

Figure 2. Raman spectrum of $[PPN]_2[Fe_4C(CO)_{12}]$ showing the symmetric M–C–M vibration ($A_1(1)$ symmetry) and lower energy M–M modes.

are three bands in the spectrum of $[Fe_4C(CO)_{12}]^{2-}$ in the region from 500 to 1000 cm^{-1} that are observed to shift on isotopic substitution of the carbide carbon with ^{13}C. Table I presents the vibrational data for this cluster and two other iron butterfly clusters of approximate C_{2v} symmetry.

A tabulation of the experimentally observed frequencies for some butterfly carbides is given in Table I. The observed shift on ^{13}C substitution of the carbide carbon is also given, along with the expected shift calculated from the values of the force constants f_1 and f_2 derived from the normal-coordinate analysis. The metal–carbon force constants f_1 and f_2 for the different butterfly carbides are listed in Table II. Although the model used in the vibrational analysis is highly simplified, there is reasonable agreement of the calculated frequencies with the observed frequencies. The greatest deviation between observed and calculated frequencies occurs for the B_1 vibrational mode. On ^{13}C substitution the metal carbide vibration of B_1 symmetry is observed to shift by approximately 7 cm^{-1} whereas the calculated shift is 20 cm^{-1}. This deviation probably arises from mixing of this mode with the M–C stretches associated with the carbonyl ligands on the cluster, which occur in the same energy region. The present calculation does not take these interaction terms into account. Despite many serious attempts, we were unable to confirm the assignments of these high-frequency Fe–C modes by the determination of Raman depolarization ratios.

Vibrational Assignments for Clusters with Lower Symmetry: $HFe_4(CH)(CO)_{12}$ and Mixed-Metal $M_3M'C$ Clusters. The clusters discussed so far have approximate C_{2v} symmetry. It is of interest

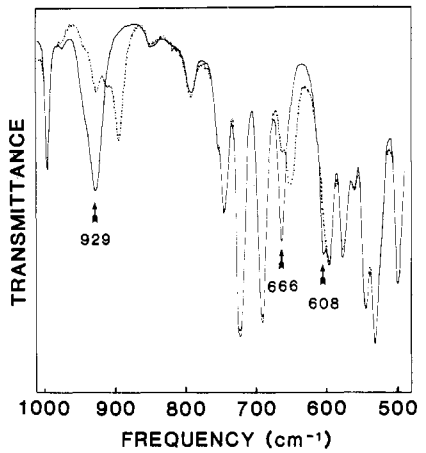

Figure 3. Infrared spectrum of $[PPN]_2[Fe_4C(CO)_{12}]$ in CsI. The solid line is natural isotopic abundance. The dotted line represents $[Fe_4C(CO)_{12}]^{2-}$ that has been isotopically enriched with ^{13}C at the carbide position.

Table II. Calculated Approximate Force Constants (N m^{-1}) for M_4C Clusters

compd	f_1	f_2
$[PPN]_2[Fe_4C(CO)_{12}]$	280	230
$[PPN][HFe_4C(CO)_{12}]$	270	230
$Fe_4C(CO)_{13}$	280	220
$HFe_4(CH)(CO)_{12}$	220	250
$[PPN][Fe_3RhC(CO)_{12}]$	290	
$[PPN]_2[Fe_3WC(CO)_{13}]$	260	

to consider the case of butterfly carbides with C_s symmetry because this point group includes two important types of carbide clusters. The first of these is the methyne cluster $HFe_4(CH)(CO)_{12}$:

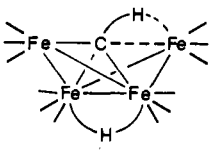

This compound is derived from $[Fe_4C(CO)_{12}]^{2-}$ by protonation.[23] It has been shown that, on prolonged exposure to strong acid, methane is evolved, the source of carbon being the carbide atom.[20] Therefore, $HFe_4(CH)(CO)_{12}$ provides a model for the cluster-based conversion of CO to methane.

A second interesting class of carbide clusters with C_s symmetry is the mixed-metal carbides. Examples of this type are $[Fe_3RhC(CO)_{12}]^-$,[22] $[Fe_3MnC(CO)_{13}]^-$,[22] and $[Fe_3MC(CO)_{13}]^{2-}$ (M = Cr, W).[27] In all cases studied to date, the heteroatom occupies

(27) Kolis, J. W.; Holt, E. M.; Hriljac, J. A.; Shriver, D. F. *Organometallics* **1984**, *3*, 496.

Table III. Carbide Vibrational Frequencies for Molecules of C_s Symmetry[a]

$HFe_4(^{12}CH/^{13}CH)(CO)_{12}$		$[PPN][Fe_3Rh-C(CO)_{12}]$		$[PPN]_2[Fe_3W-C(CO)_{13}]$	
freq, cm^{-1}	mode	freq, cm^{-1}	mode	freq, cm^{-1}	mode
824/800	A′(3)	953	A″	899	A″
657/645	A′(2)	668	A′(2)	651	A′(2)
	A″		A′(3)		A′(3)
248[b]	A′(1)	274[b]	A′(1)	263[b]	A′(1)

[a] All vibrational frequencies were measured in Nujol mulls by IR except as noted. [b] From Raman spectroscopy of polycrystalline samples.

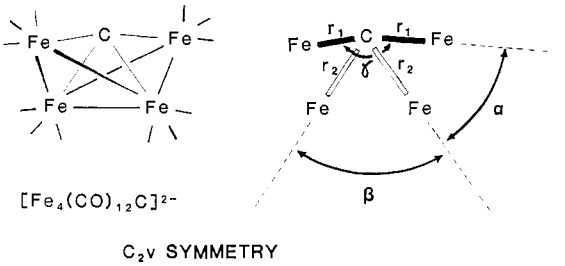

Figure 4. Model used in the simple valence force field calculation to determine energy ordering of the vibrational modes and the associated M–C force constants in molecules of approximate C_{2v} symmetry.

a hinge position in the cluster, as depicted in Figure 6. The mixed-metal carbides show reactivity different from that of the homometallic analogue.[22]

Qualitatively the spectra of the carbides of C_s symmetry are similar to those of the carbides of C_{2v} symmetry (Table III). Hence, the highest energy carbide mode is readily observed as a strong band in the infrared spectrum between 800 and 1000 cm^{-1}. Similarly, the A′ ($A_1(2)$ in C_{2v}) vibration around 650 cm^{-1} is easily discerned. The lowest energy carbide mode is also readily observed as an intense band in the Raman spectrum between 240 and 300 cm^{-1}.

The remaining vibrational mode is difficult to observe experimentally. On the basis of the simple valence force field calculation, the frequency of this vibration is expected around 600 cm^{-1}. As previously mentioned, this is in the region of metal–carbon M–CO stretches, so this mode can often be obscured by or mixed in with these vibrations.

Table III lists the vibrational frequencies and their assignments for some metal carbide clusters of approximate C_s symmetry. The energy ordering of these modes follows the ordering in the corresponding clusters of C_{2v} symmetry. In all of the butterfly carbides for which crystallographic data are available, the wing-tip–carbide distances are significantly shorter than the hinge–carbide distances (Table IV). The result is that the force field acting on the carbide atom is similar in all cases, leading to analogous spectral patterns.

The high-energy A′ mode of $HFe_4CH(CO)_{12}$, at 824 cm^{-1}, is significantly lower than the typical value of ca. 900 cm^{-1} found in the other carbides studied. This can be understood by examining the nature of the A′ vibration. As shown in Figure 1, the highest energy vibrational mode in these four-coordinate carbides involves motion of the carbon atom between the two wing-tip atoms of the cluster. The agostic interaction of the CH group of $HFe_4(CH)(CO)_{12}$ with one of the wing-tip iron atoms presumably affects that Fe–C force constant significantly. It follows from the valence force field calculation that to a first approximation the high-energy A′ mode should be most affected by a modification to the wing-tip–carbide force constant f_1, and qualitatively that is what is observed. Thus, on comparison of the carbide vibrations of $[HFe_4C(CO)_{12}]^-$ with the vibrations of $HFe_4(CH)(CO)_{12}$, the high-energy wing-tip–carbide–wing-tip mode (B_2 and A′, respectively) is shifted by almost 100 cm^{-1}, whereas the other observed carbide modes of the two complexes differ by less than 30 cm^{-1}.

The large shift in the highest energy A′ vibration is reflected in the force constant associated with the (η^2-CH)–Fe interaction (f_2), which is less than that for a carbide–wing-tip Fe interaction (f_1; see Table II).

A general trend in the force constants associated with the butterfly carbide M–C bonds is that the carbide to wing-tip metal force constants are larger than the carbide to hinge metal force constants. As mentioned previously, this is a reflection of the significantly shorter carbide to wing-tip metal bond distances. The hinge metal to carbide carbon force constants observed in the tetrairon butterfly clusters are slightly higher than the force constants derived in a similar manner for interstitial carbide clusters with six to eight metal atoms surrounding the carbon atom (range 80–200 N m^{-1}).[11,12,15,17] However, the force constants associated with the wing-tip metal to carbide carbon bonds are ca. 280 N m^{-1}. This uniquely high force constant found in the butterfly carbides accounts for the observation of the highest frequency carbide mode in the 900-cm^{-1} region. The highest frequency carbide vibration for penta- and hexametal carbides appears in the 800-cm^{-1} region.[9,13,15,17]

Calculation of Force Constants. Wilson's **F–G** matrix method[26] was employed to calculate approximate metal–carbon force constants and infer the correctness of the spectral assignments. The calculation was performed on a model system of four iron atoms and a carbon atom in a butterfly arrangement of C_{2v} symmetry. Symmetry-averaged bond angles and distances were taken from the X-ray crystal structures of each compound (Table IV). A simple valence force field based exclusively on bond stretching coordinates was employed. Two separate force constants were employed because the X-ray crystal structures indicate that the $Fe_{wing\text{-}tip}$–C bond distances are significantly shorter than the Fe_{hinge}–C distances. For each cluster one force constant was determined for the $Fe_{wing\text{-}tip}$–C–$Fe_{wing\text{-}tip}$ interaction and another for the Fe_{hinge}–C–Fe_{hinge} bonds (Figure 4). In view of the difference in bond distances the $Fe_{wing\text{-}tip}$–C force constant f_1 is expected to be larger in magnitude than the Fe_{hinge}–C force constant f_2. This view is consistent with the results of a Fenske–Hall molecular orbital calculation on $[Fe_4C(CO)_{12}]^{2-}$, from which the overlap between the carbide atom and a wing-tip iron is calculated to be 1.5 times that between the carbide and the hinge iron.[28]

Table IV. Crystallographic Data Used in Calculation of M–C Force Constants

compd	$M_{wing\text{-}tip}$–C dist, Å	M_{hinge}–C dist, Å	α, deg	β, deg	γ, deg	α′, deg	ref
$[Fe_4C(CO)_{12}]^{2-}$	1.80	1.96	89	81	176		*b*
$[HFe_4C(CO)_{12}]^-$	1.79	1.99	88	82	174		*c*
$Fe_4C(CO)_{13}$	1.80	1.99	88	79	175		*d*
$HFe_4(CH)(CO)_{12}$	*a*	*a*	85	84	171	88	*e*
$[Fe_3RhC(CO)_{12}]^-$	1.77	2.09	88	78	173	87	*f*
$[Fe_3WC(CO)_{13}]^{2-}$							*g*

[a] The model for $HFe_4(CH)(CO)_{12}$ consists of three long M–C vectors of 1.94 Å and one short M–C vector ((η^2-CH)–Fe) of 1.83 Å (see Figure 6). [b] Boehme, R. F.; Coppens, P. *Acta Crystallogr., Sect. B: Struct. Crystallogr. Cryst. Chem.* **1981**, *B37*, 1914. [c] Reference 20. [d] Reference 21. [e] Beno, M. A.; Williams, J. M.; Tachikawa, M.; Muetterties, E. L. *J. Am. Chem. Soc.* **1980**, *102*, 4542. [f] Reference 22. [g] There are no crystallographic data available for $[Fe_3WC(CO)_{13}]^{2-}$; the relevant parameters for $Fe_4C(CO)_{13}$ were used.[20]

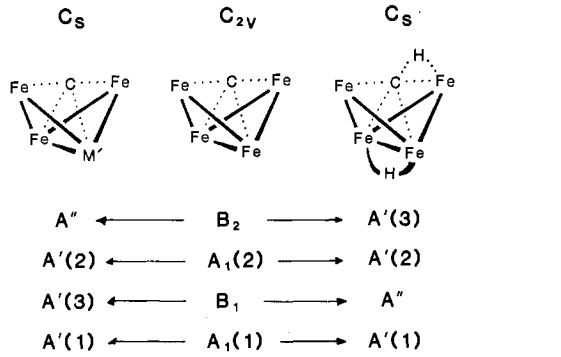

Figure 5. Correlation diagram showing the vibrational assignment of the four carbide modes on lowering the symmetry of the cluster from C_{2v} to C_s.

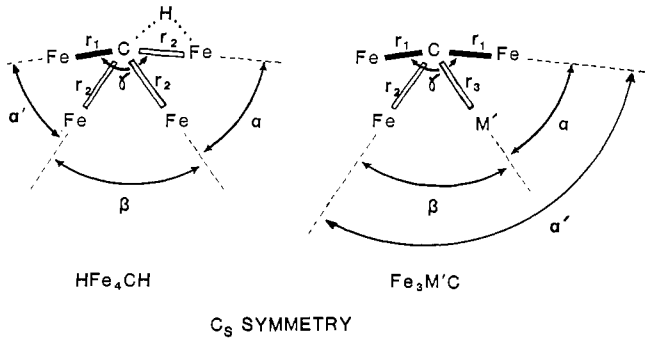

Figure 6. Model used in the simple valence force field calculation to determine the M–C force constants in butterfly carbides of approximate C_s symmetry.

The calculated energy ordering of the Fe–C vibrational modes based on the model described above is

$$\nu(B_2) > \nu(A_1(2)) > \nu(B_1) \gg \nu(A_1(1))$$

and the expected ratios between the frequencies are

$$\nu(A_1(2))/\nu(B_1) = \text{ca. } 1.2$$

$$\nu(B_2)/\nu(A_1(1)) = \text{ca. } 3.2$$

On introduction of a heteroatom into the metal framework or in the methyne cluster $HFe_4(CH)(CO)_{12}$, the symmetry is reduced to C_s. The number of metal carbide vibrational modes predicted in this point group, as in C_{2v}, is four. There are three of symmetry A′ and one of symmetry A″, as shown in the correlation diagram of Figure 5. The A″ mode is derived from either the B_2 or the B_1 mode under C_{2v}, depending on which mirror plane is destroyed on lowering to C_s. Additionally, the mixed-metal system must now be described in terms of three force constants instead of two.

For the purpose of a vibrational analysis of the metal carbide portion of these clusters, the CO ligands were neglected and a simple valence bond stretching potential function was assumed:

$$2V = f_1(\Delta r_1)^2 + f_2(\Delta r_2)^2$$

where r_n values are the internal coordinates depicted in Figures 4 and 6 and f_n values are the associated force constants. The determinants solved and relevant variables used in the normal-coordinate analysis are given in the supplementary material.

Angles and bond distances were obtained from published crystallographic data. Values of the metal–carbon force constants were obtained by approximate solution of the determinantal equations. In Table I the calculated values of the frequencies associated with the molecules were determined on the basis of force constants derived from the measured frequencies. The force constants listed in Table II are calculated on the basis of a least-squares fit of the isotopic data available for the two highest frequency carbide vibrations (i.e. the bands in the 900- and 650-cm^{-1} regions) because these are the purest modes and so yield the most reliable force constants. The second and third force constants acting on the mixed-metal carbides of C_s symmetry were not calculated because of our inability to reliably observe the additional M–C vibrational frequencies associated with these force constants.

(28) Harris, S.; Bradley, J. S. *Organometallics* **1984**, *3*, 1086.

Table V. ν(M–N) Vibrational Assignments

compd	β, deg	$\nu(B_1)$, cm^{-1}	$\nu(A_1(2))$, cm^{-1} obsd	$\nu(A_1(2))$, cm^{-1} calcd
$Ru_4N(CO)_{12}(\mu\text{-H})$	83	[623 (vs), 621 (vs)]	685 (m)	693
$Ru_4N(CO)_{11}(\mu\text{-H})_3$	86	633 (s)	676 (m)	673
$Ru_4N(CO)_{12}(\mu\text{-NCO})$	97	706 (mw)	595 (vs)	634
$Ru_4N(CO)_{12}(\mu\text{-NO})$	106	[740 (w, sh), 734 (w)]	591 (vs)	576

[a] All experimental data taken from ref 29.

The assignment of the symmetry species for the various carbide vibrational modes was based on the simple valence force field calculation described above and was confirmed in part by polarization data from Raman spectroscopy. A different set of assignments has recently been reported for a series of butterfly nitride clusters where modes associated with the nitride ligand were considered.[29] The criterion used to assign two of the four M–N stretching modes was based on changes in frequency for a series of butterfly nitrides having different geometries. For compounds having the formula $Ru_4N(CO)_{12}(\mu\text{-L})$ the value of the angle β (Figure 4) increases on going from L = H to NCO to NO. It was argued that as β increases the frequency for the B_1 mode should increase and that for the A_1 mode should decrease. This qualitative argument is borne out by the present vibrational analysis, which yields the following expressions for the frequencies:

$$\nu(A_1(2)) = [k(\mu_N(1 + \cos\beta) + \mu_{Ru})f_2]^{1/2} \qquad \alpha \approx 90° \quad (1)$$

$$\nu(B_1) = [k(\mu_N(1 - \cos\beta) + \mu_{Ru})f_2]^{1/2} \quad (2)$$

From these expressions it can be seen that an increase in the value of β (for $0° < \beta < 180°$) will lead to an increase in $\nu(B_1)$ and a decrease in $\nu(A_1)$, as was predicted qualitatively. However, these frequency trends do not provide an unambiguous assignment of the observed spectrum. From eq 1 and 2 the ratio of frequencies of the vibrational modes of A_1 and B_1 symmetry are given by eq 3. For compounds with β angles less than 90° the $A_1(2)$ mode

$$\frac{\nu(B_1)}{\nu(A_1(2))} = \left[\frac{\mu_N(1 - \cos\beta) + \mu_{Ru}}{\mu_N(1 + \cos\beta) + \mu_{Ru}}\right]^{1/2} \quad (3)$$

is predicted to be higher in energy than the B_1 mode, and this order is predicted to switch for compounds with β angles greater than 90°. Thus, we are inclined to interchange the assignment of the 685- and 621/623-cm^{-1} bands for $Ru_4N(CO)_{12}(\mu\text{-H})$, which brings them into closer agreement with eq 3 (Table V). Table V also lists the calculated values of the frequencies of the $A_1(2)$ symmetry modes based on the experimental values of the B_1 modes. The experimental values of Table V are all taken from ref 29. The two compounds that we have reassigned are $Ru_4N(CO)_{11}(\mu\text{-H})_3$ and $Ru_4N(CO)_{12}(\mu\text{-H})$, which both have β's less than 90°. Solution Raman polarization data could serve to confirm these assignments, as the totally symmetric $A_1(2)$ mode is expected to be polarized while the B_1 mode would be depolarized. We were, however, unable to obtain Raman spectra of the iron carbides above ca. 400 cm^{-1} because they are very weak Raman scatterers.

Conclusions

Infrared bands associated with the carbon atom in the exposed four-coordinate "butterfly" environment of iron carbonyl clusters

(29) Anson, C. A.; Attard, J. P.; Johnson, B. F. G.; Lewis, J.; Mace, J. M.; Powell, D. B. *J. Chem. Soc., Chem. Commun.* **1986**, 1715. Because of a different choice of coordinates, the modes assigned to B_1 in the present paper correspond to B_2 of Anson et al. and likewise B_2 of the present work corresponds to B_1 of Anson et al.

are distinct from the carbide modes for encapsulated carbide ligands. The compounds display a strong carbide vibration in the 900-cm^{-1} region of the infrared spectrum, indicating a butterfly carbide geometry and corresponding to vibration of the carbon atom between the two wing tips of the butterfly. This band is readily observed because it appears in a spectral region that is clear of any other cluster or PPN^+ (PPN^+ = bis(triphenylphosphine)nitrogen(1+)) counterion vibrational modes. The corresponding carbide modes for penta- and hexametal carbides appear at lower frequency, usually around 800 cm^{-1}.[9,13,15]

The force constants, calculated by means of a simple bond stretching force field with neglect of CO ligands, are largest for the wing-tip iron to carbon bonds and are not sensitive to the charge on the cluster. The force constants for both the carbide–wing-tip metal and carbide–hinge metal interactions in these four-metal butterfly clusters are larger than the carbide–metal force constants in metal clusters having six- and eight-coordinate carbide.[11] Apparently, this trend reflects the more delocalized C–M bonding in the latter clusters.

Acknowledgment. Research conducted at Northwestern University was supported by NSF Grant CHE-8506011 and DOE Grant DE-AC02-83ER13104. P.L.S. acknowledges support by an MPI Grant 40% Fund.

Supplementary Material Available: Tables of IR data for the compounds reported from 1000 to ca. 500 cm^{-1} and of determinants used in the approximate normal-coordinate analysis (4 pages). Ordering information is given on any current masthead page.

Contribution from the Department of Chemistry and Laboratory for Molecular Structure and Bonding, Texas A&M University, College Station, Texas 77843, and Department of Chemistry and Biochemistry, Southern Illinois University, Carbondale, Illinois 62901

Reactions of Small Molecules with $Re_2Cl_4(PEt_3)_4$. 2.[1] Products Resulting from the Reaction with Dihydrogen

S. Bucknor,[2a] F. A. Cotton,*[2b] L. R. Falvello,[2b] A. H. Reid, Jr.,[2b] and C. D. Schmulbach*[2a]

Received February 4, 1987

Treatment of $Re_2Cl_4(PEt_3)_4$ with H_2, carried out in dichloromethane for 24 h under a pressure of 120 atm, gave no result, but when the temperature was raised to 60 °C and maintained there for 7 days, about 44% of the $Re_2Cl_4(PEt_3)_4$ reacted to afford, reproducibly, three products, separable by chromatography on silica gel. These were red *trans*-$ReCl_4(PEt_3)_2$ (a known compound), yellow-brown $[PEt_4][Re_2Cl_6(PEt_3)_2H]$ (**1**, a new compound and the major product), and yellow-green $[PEt_4][ReCl_5(PEt_3)]$ (**2**, a new compound). The two new compounds were each identified and their structures determined by X-ray crystallography. In one run there were also a few pink crystals that could be only incompletely characterized crystallographically as perhaps $ReCl_3(PEt_3)_2H$. Crystallographic data: for **1**, $P2_1/a$ with a = 15.937 (9) Å, b = 12.101 (4) Å, c = 17.496 (15) Å, β = 93.41 (6)°, and Z = 4, refined to R = 0.0390 and R_w = 0.049; for **2**, $P2_1/m$ with a = 9.951 (2) Å, b = 10.147 (2) Å, c = 11.637 (2) Å, β = 91.04 (2)°, and Z = 2, refined to R = 0.0487 and R_w = 0.0609. Compound **1** contains a confacial bioctahedral anion, $[Cl_2(Et_3P)Re(\mu\text{-}H)(\mu\text{-}Cl)_2ReCl_2(PEt_3)]^-$, which has effective C_2 symmetry. The Re–Re distance is 2.349 (1) Å, and the end-to-end symmetry of the heavy atom structure suggests that the μ-H atom is symmetrically placed, i.e., on the effective C_2 axis of symmetry. The $[ReCl_5(PEt_3)]^-$ ion resides on a mirror plane and has effectively C_{4v} symmetry in the coordination sphere.

Introduction

The reaction patterns of Re(II) compounds containing the electron-rich ($\sigma^2\pi^4\delta^2\delta^{*2}$) Re–Re triple bond are varied and, in many instances, complex.[3] Carbonylation of $Re_2Cl_4(PR_3)_4$ compounds characteristically occurs with metal–metal bond cleavage accompanied by oxidation and/or reduction.[1,4-6] In the exceptional case involving $Re_2Cl_4(\mu\text{-dppm})_2$, carbonylation occurs with retention of the multiple Re–Re bond, but other bonds are rearranged to give $Cl_2Re(\mu\text{-}Cl)(\mu\text{-}CO)(\mu\text{-dppm})_2ReCl(CO)$.[7] In contrast, oxidation of Re_2^{4+} complexes by methanolic HCl or elemental oxygen occurs with retention of both the Re–Re multiple bond and the eclipsed conformation of the starting material. The compound $Re_2Cl_4(PEt_3)_4$ is oxidized to $Re_2Cl_6(PEt_3)_2$ by methanolic HCl, and the oxidation of $Re_2Cl_4(PR_3)_4$ complexes by elemental oxygen gives $Re_2X_4(PR_3)_4^+$ and/or their neutral $Re_2X_5(PR_3)_3$ analogues.[8-10]

We report here the first study of the reaction of $Re_2Cl_4(PEt_3)_2$, a well-characterized member of a class of compounds containing an electron-rich Re_2^{4+} core,[11] with elemental hydrogen. The reaction pattern observed for hydrogenation in dichloromethane is unlike those reported for other small gaseous molecules. Because the hydrogenation reaction is relatively slow, experiments were conducted at elevated pressures with apparatus and techniques described earlier.[12]

Experimental Section

Purification of Solvents. Dichloromethane and acetonitrile were dried by refluxing for 8 h over phosphorus pentoxide under a blanket of nitrogen. The solvents were then distilled under nitrogen into another flask containing phosphorus pentoxide. After the solvents were degassed by using several freeze/thaw cycles, the solvents were refluxed under nitrogen for 17 h. Samples were fractionally distilled immediately prior to use. Hexane and tetrahydrofuran were predried over sodium for several weeks and distilled onto fresh sodium/benzophenone under nitrogen. The solvents were degassed and refluxed until the color of the benzophenone ketyl radical anion persisted.

Reagents. Hydrogen gas (Linde, ultrahigh purity) and deuterium (Matheson, CP grade, 99.5 atom % minimum) were used without further purification. Argon (Linde, prepurified) was passed through a Model 98HP purifier (Airco), to remove traces of oxygen and water.

(1) Part 1: Bucknor, S.; Cotton, F. A.; Falvello, L. R.; Reid, A. H., Jr.; Schmulbach, C. D. *Inorg. Chem.* **1986**, *25*, 1021.
(2) (a) Southern Illinois University. (b) Texas A&M University.
(3) (a) Walton, R. A. *ACS Symp. Ser.* **1981**, *155*, 212-217. (b) Cotton, F. A.; Walton, R. A. *Multiple Bonds Between Metal Atoms*; Wiley: New York, 1982; Chapter 5.
(4) Hertzer, C. A.; Myers, R. E.; Brant, P.; Walton, R. A. *Inorg. Chem.* **1978**, *17*, 2383.
(5) Dunbar, K. R.; Walton, R. A. *Inorg. Chim. Acta* **1984**, *87*, 185.
(6) Bucknor, S. Doctoral Dissertation, Southern Illinois University, Carbondale, IL, 1985.
(7) Cotton, F. A.; Daniels, L. M.; Dunbar, K. R.; Falvello, L. R.; Tetrick, S. M.; Walton, R. A. *J. Am. Chem. Soc.* **1985**, *107*, 3524.
(8) Ebner, J. R.; Walton, R. A. *Inorg. Chem.* **1975**, *14*, 1987.
(9) Glicksman, H. D.; Walton, R. A. *Inorg. Chem.* **1978**, *17*, 3197.
(10) Ebner, J. R.; Walton, R. A. *Inorg. Chim. Acta* **1975**, *14*, L45.
(11) Cotton, F. A.; Frenz, B. A.; Ebner, J. R. Walton, R. A. *Inorg. Chem.* **1976**, *15*, 1630.
(12) Ballintine, T. A.; Schmulbach, C. D. *J. Orgamomet. Chem.* **1979**, *164*, 381.

0020-1669/87/1326-2954$01.50/0